論 文

[2180] BENDING PERFORMANCE OF CENTRIFUGED PRECAST COLUMNS WITH LAPPING JOINTS

Rodolfo YANEZ*, Teruaki YAMAGUCHI** and Hiroshi IMAI***

ABSTRACT

To investigate the performance of a newly developed joint method, six full scale columns with and without joints were subjected to inelastic cyclic loads under constant axial forces. The joints used herein were lapping joints developed for Precast Concrete (PCa) columns. From load-displacement, moment-curvature, and shear stress-shear distortion curves, no much differences between specimens with and without joints were appreciated, showing a good performance of the proposed joint.

1. INTRODUCTION

At the present, mortar grouted steel sleeve joints are commonly used in PCa columns in Japan. This joint needs special devices, technicians and are located at the member ends where the stresses due to seismic forces are large. A cheaper and simple bar joint method has been developed, which is located at the mid-height of columns, where the stresses are small. In the reinforcing cage, steel sheaths are placed at the position of main bars, and lapped with two bars each. Concrete is cast and compacted by centrifugation. At the construction site the main bars are inserted into the sheaths, so the end of each bar abuts at the center of lapping bars. The core concrete is cast and high strength mortar is grouted inside the sheaths. This joint is classified into one of lapping joints. Since the bond performance of the system influenced over the joint characteristics, pull out test on columns with different conditions was carried out [1]. However the seismic behavior of columns with joints, under severe bending stress, are not clear because the stress condition of jointed bars is a little different from those under pull out tests.

2. SPECIMENS

Figure 1 illustrates the specimen geometry and Table I summarizes the properties of column specimens. Cantilever type columns were used to apply

* Doctoral Degree Program, University of Tsukuba
** Technical Research Institute, Kabuki Construction Co. Ltd.
*** Institute of Engineering Mechanics, University of Tsukuba

severe bending stress at the jointed portion. Test specimens were representative of the first story columns of low-rise buildings in Japan. Each Specimen consists of a column, top and footing beams. The column has a cross section of 600 mm by 600 mm. Specimen RC-1 was a monolithic reinforced concrete column. Specimens PC-1 and PC-2 were precast concrete columns with continuous main bars. Specimens PC-3, PC-4, and PC-5 were precast concrete columns with the joint at the bottom. The PCa part was compacted by centrifuging at 16800 RPM for about 20 minutes, then cured under steam of 70°C for one night. Once the lower half of the column main bars (screw type deformed bars) were placed in the footing beam, the precast column was lifted down inserting the projecting main bars into the sheaths from the bottom of the column and supported with nuts and steel plates at the corners. The clearance of the bottom was 5 cm high. The other half main bars were inserted from the top, and the upper precast beam (with no concrete at the central part), was placed and the concrete (central part of column and upper beam) was cast in. Then high strength mortar was grouted inside the sheaths. In order to prevent lateral slippage at the bottom of the column, due to repeated shear forces, shear cotters were provided as shown in Fig. 2. Steel properties are shown in Table II.

3. TEST APPARATUS AND INSTRUMENTATION

Lateral load was applied at 1400 mm high from the top of the footing beam, so the shear span ratio (H/D) was 2.3. Axial load was applied by two actuators with the same loads through the top beam. Horizontal displacements

Table I Properties of Specimens

Test Specimen	Concrete Strength kgf/cm²	Axial Stress kgf/cm²	Remarks
RC-1	246	30	Monolithic
PC-1	399	30	Without Joint
PC-2	418	40	Without Joint
PC-3	473	30	With Joint
PC-4	449	40	With Joint
PC-5	448	50	With Joint
Core Concrete	250		4 Weeks
Grouted Mortar	763		2 Weeks
	818		7 Weeks

Table II Steel Properties

Size	Grade	σ_y (tf/cm²)	σ_b (tf/cm²)	E (tf/cm²)
D10	SD295A	3.50	4.65	1810
D16	SD345	3.77	5.57	1800
D22		4.10	5.80	1910

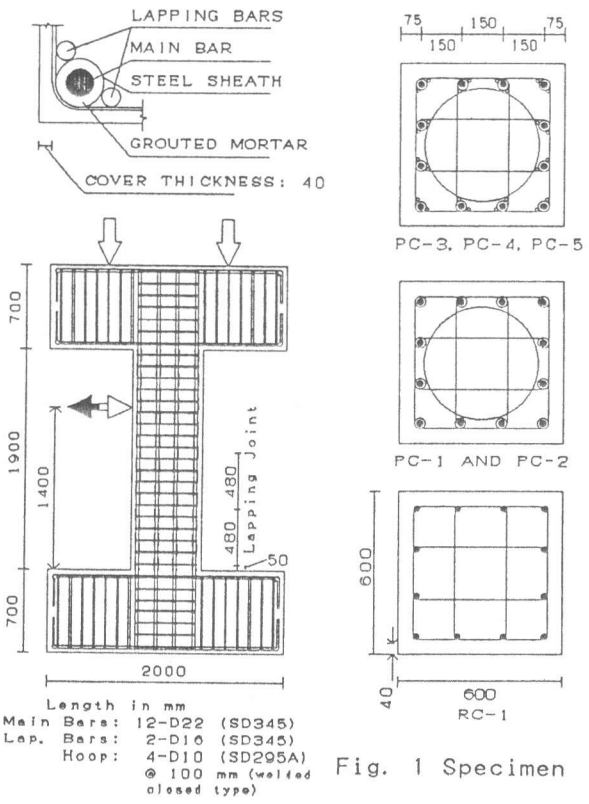

Fig. 1 Specimen

relative to the footing beam were measured at the loading points. Additional displacement transducers were placed on one face of the columns to measure rotations and shear distortions at different heights of the column as shown in Fig. 3. Steel strains were also measured. Cracks were marked when they appeared and maximum crack widths were measured when the peak displacements were reached. Figure 4 illustrates the unidirectional displacement history. The horizontal displacement angle R relative to the footing beam was controlled. The displacement angle R=±1/800 was first applied, then two cycles at R=±1/400, ±1/200, ±1/100, ±1/50 each, and finally one cycle at R=±1/25 were applied.

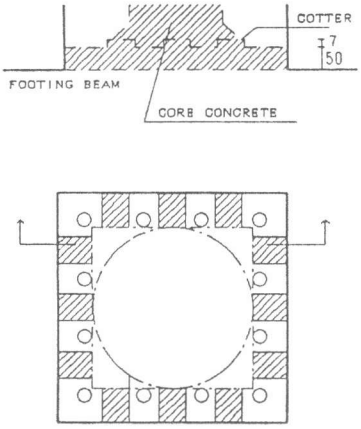

Fig. 2 Detail of Column Base

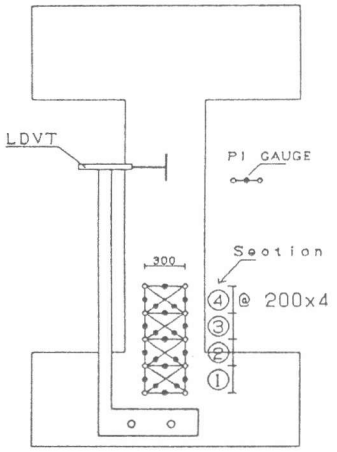

Fig. 3 Arrangement of Disp. Transducers

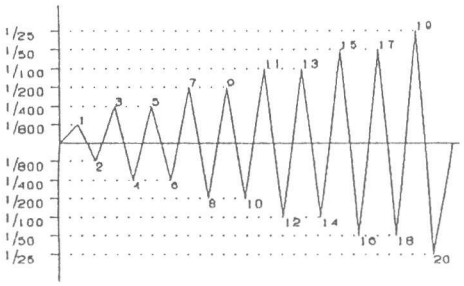

Fig. 4 Loading History

4. TEST RESULTS

4.1 CRACK PATTERNS

All the specimens developed their full flexural yield strength prior to shear failure. Cracking patterns of Specimens RC-1, PC-3 are shown in Fig. 5. Primary cracks were generally horizontal, apparently due to the flexural effects. As load increased, horizontal cracks formed on the perpendicular face to the loading direction, and diagonal cracks formed on the faces parallel to the load direction. After R=1/100, development of new cracks slowed, but at larger drift angle, crack widths of some major

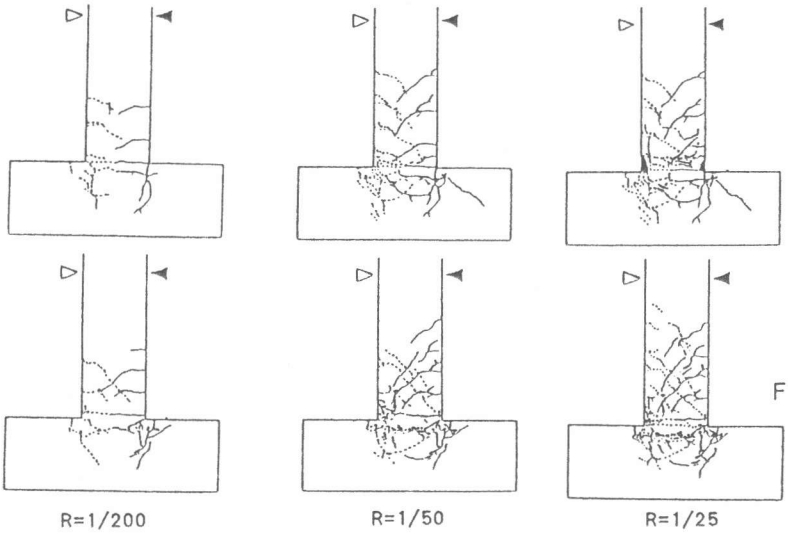

(a) Specimen RC-1

(b) Specimen PC-3

Fig. 5 Crack Patterns

existing cracks became larger. Concrete crushing was observed near the column base. The spalling of concrete did not begin until R= 1/50.

4.2 LATERAL LOAD-DISPLACEMENT RELATIONS

Figure 6 illustrates the lateral load-displacement (Q-δ) relations for Specimens RC-1, PC-1 and PC-3. Lateral loads presented here were already corrected by the lateral component of axial load. Twist of the column about the column axis was neglible. The ultimate moment was calculated using the Eq. (1):

$$M_u = \Sigma \left\{ 0.9 \cdot a_t \cdot \sigma_y \cdot d + 0.5 \cdot N \cdot D \cdot \left(1 - \frac{N}{b \cdot D \cdot Fc} \right) \right\} \qquad (1)$$

where

a_t, σ_y = sectional area and yield stress of tensile bars
b, D, d = width, total depth, and effective depth of column
N = axial force
Fc = compressive strength of concrete

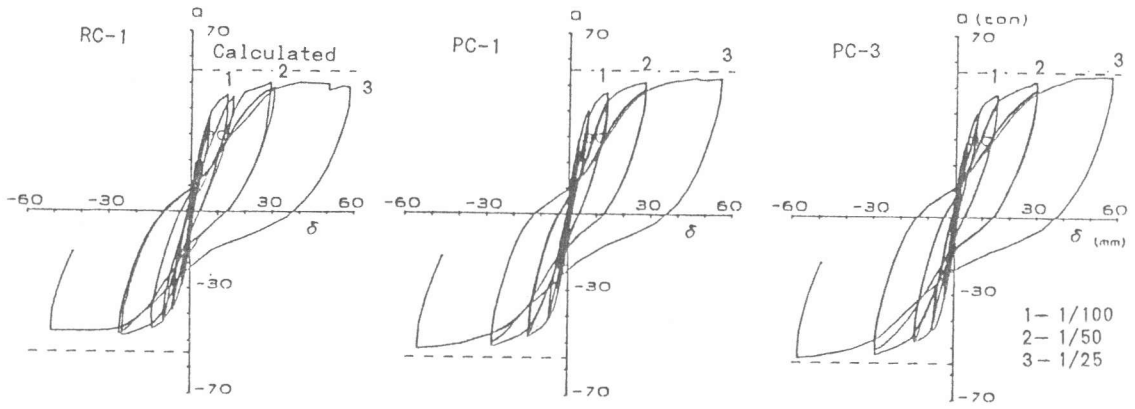

Fig. 6 Lateral Load-Displacement

The envelope curves of load-displacement responses are shown in Fig. 7. All specimens showed a good hysteretic behavior. Specimens PC-1 and and PC-3 with axial stress of 30 kgf/cm^2; and PC-2 and PC-4 with axial stress of 40 kgf/cm^2, showed almost the same hysteretical patterns for each of the pairs. All specimens yielded at R=1/100, and after R=1/50 a

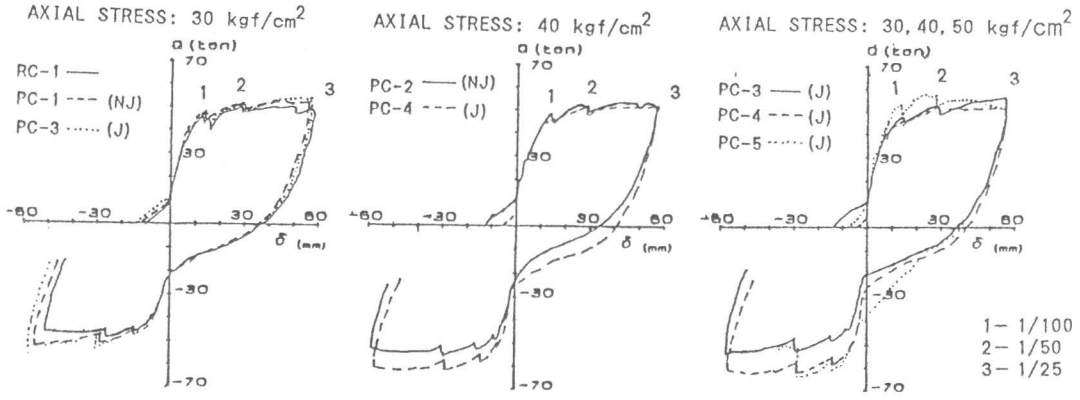

Fig. 7 Envelope Curves of Load-Displacement Responses

decrement in the stiffness was appreciated. The effects of the lapping bars and the high strength mortar were predominant. This means the system lapping bar-sheath-mortar-main bar behaved like one element. Calculated and experimental values of ultimate bending capacities are shown in Table III. They show a good agreement and these values did not change even though the axial stress was increased.

Table III Ultimate Capacity

Specimen	Muc t-m	Mue t-m	Mue / Muc
RC-1	76.37	70.39	0.92
PC-1	77.89	74.12	0.95
PC-2	86.99	77.48	0.89
PC-3	78.27	76.48	0.98
PC-4	87.28	87.39	1.00
PC-5	95.90	89.46	0.93

4.3 MOMENT-CURVATURE RELATIONS

Figure 8 illustrates the moment defined at the bottom of column versus the curvature at different heights of the column for Specimens PC-1 and PC-3. Base moments were already corrected due to the effect of the axial loads. The curvature distributions show that the deformation is concentrated on Section 2, which is the hinging region, and that all specimens have the same moment-curvature patterns in each section.

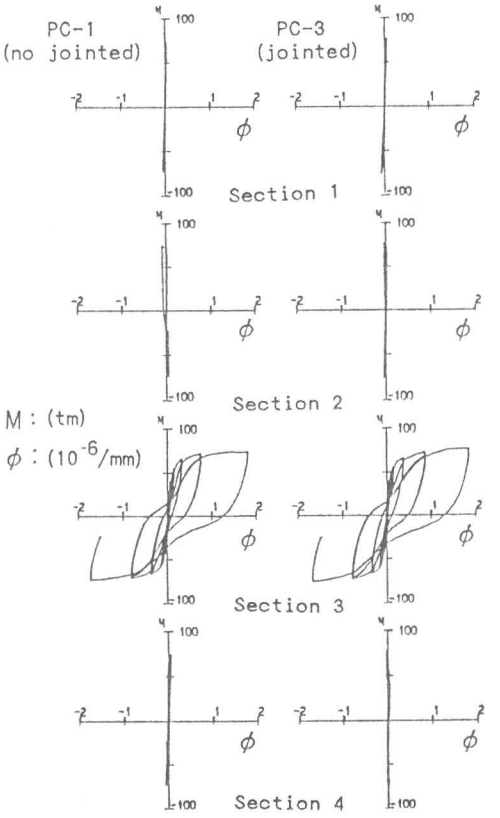

Fig. 8 Moment-Curvature Relations

4.4 SHEAR STRESS-SHEAR DISTORTION RELATIONS

Figure 9 illustrates the shear stress-shear distortion relations for Specimens PC-1 and PC-3. Shear distortion is very small at every section of the columns. But at the bottom, where the joint was located, the shear distortion became larger at the last stage, because the shear distortion defined from two diagonal deformations include the effect of the bending deformation of the plastic hinge. No slippage of columns respect to the footing is recognized.

4.5 STRAIN DISTRIBUTIONS

Strain distributions indicate that in all specimens the initial yielding started at R=1/100 for the main bars, and no yielding was observed in lapping bars, as shown in Fig. 10. It is also observed that jointed main bars of Specimen PC-4 showed smaller strains than those with continuous main bars in Specimen PC-2. When the strains of the lapping bars are added to the strain of the corresponding jointed main bars, the difference between strains of main bars, with and without joints, became

smaller. Therefore, it might be acceptable that the joint system showed a good performance in order to transfer the full strength of the main bars.

5. CONCLUSIONS

From the foregoing discussions, the following conclusions can be obtained.

1) Not much differences were observed between the monolithic and the other PCa specimens except for crack patterns.
2) Not much differences were observed between the PCa specimens with and without joints in the load-deformation curves.
3) No slippage of column respect to the footing beam can not be recognized from the shear stress-shear distortion curves.
4) All specimens yielded in flexure at the column base and lateral strengths agreed well to those based on the calculated flexural capacities.

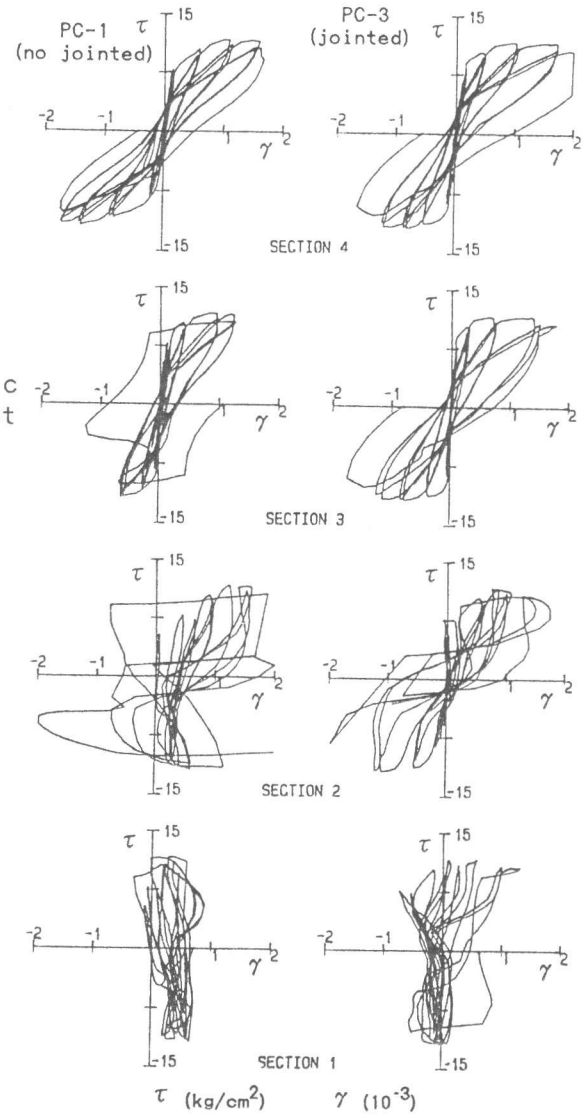

Fig. 9 Shear Stress- Shear Distortion Relations

REFERENCES

1) Imai H., Yamaguchi T., Yanez R., "Bond Performance of a Lapping Joint Developed for Precast Concrete Columns", Proceedings of The Japan Concrete Institute, Vol. 13, No. 2, to be published.

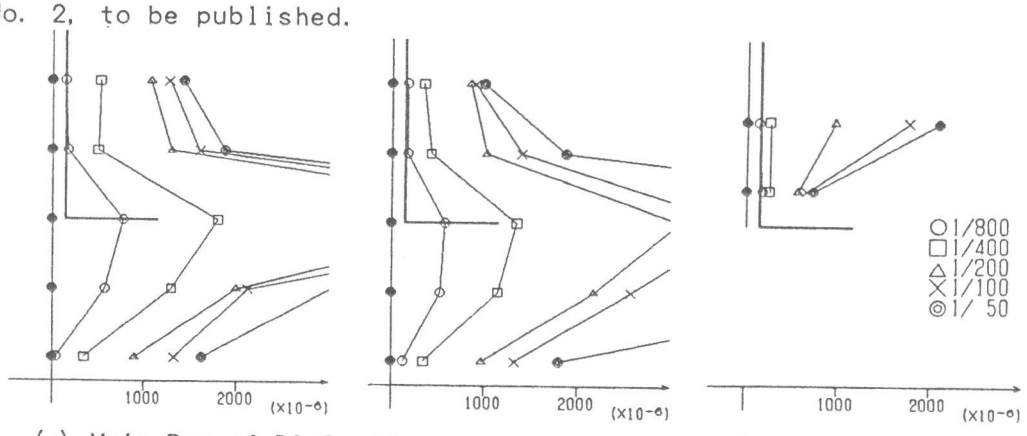

(a) Main Bar of PC-2 (b) Jointed Bar of PC-4 (c) Lapping Bar of PC-4

Fig. 10 Strain Distributions of Main and Lapping Bars